Tunneling site of electrons in strong-field-enhanced ionization of molecules

Cheng Huang,[1,2] Pengfei Lan,[1,*] Yueming Zhou,[1] Qingbin Zhang,[1] Kunlong Liu,[1] and Peixiang Lu[1,†]

[1]*School of Physics and Key Laboratory of Fundamental Physical Quantities Measurement of Ministry of Education, Huazhong University of Science and Technology, Wuhan 430074, People's Republic of China*

[2]*School of Physics, Southwest University, Chongqing 400715, People's Republic of China*

(Received 2 December 2013; published 31 October 2014)

We investigated electron emissions in strong-field-enhanced ionization of asymmetric diatomic molecules by quantum calculations. It is demonstrated that the widely used intuitive physical picture, i.e., electron wave-packet direct ionization from the up-field site (DIU), is incomplete. Besides DIU, we find another two ionization channels: the field-induced excitation with subsequent ionization from the down-field site and that from the up-field site. The contributions from these channels depend on the molecular asymmetry and internuclear distance. Our work provides a more comprehensive physical picture for the long-standing issue about enhanced ionization of diatomic molecules.

DOI: 10.1103/PhysRevA.90.043420 PACS number(s): 32.80.Rm, 31.90.+s, 32.80.Fb

I. INTRODUCTION

Tunneling ionization is one of the most fundamental quantum effects when atoms and molecules are exposed to a strong laser field. As the doorway step of various strong-field processes, such as high-order harmonic and attosecond pulse generation [1,2], double ionization [3,4], and above-threshold ionization [5,6], understanding the ionization dynamics is of essential importance for controlling the electron dynamics in these processes. Moreover, the molecular ionization signal itself also preserves some information of the molecular structure and thus can be used to image molecular structure [7,8]. Therefore, the ionization has attracted significant interest over the past several decades. Theories, including positive partial transpose [9] and Ammosov-Delone-Krainov [10], have been well established for atoms. Many efforts have also been made to extend these theories to molecules [11]. Nevertheless, because the molecules have more degrees of freedom and more complicated structures, the underlying physics becomes richer and the ionization dynamics is still not completely clear. It has been demonstrated that when the molecule is stretched to a critical internuclear distance R_c the ionization probability sharply increases, which is called enhanced ionization (EI) [12–19]. An intuitive physical picture [12–14] based on the quasistatic tunneling theory [20] has been proposed to explain the behavior of molecular EI. When the molecule is stretched to the critical distance R_c, an inner potential barrier between the two cores emerges and localizes the electron population at each of the cores. Then, the up-field population only needs to tunnel through the inner barrier directly to the continuum, which is considerably easier than tunneling through the outer barrier between the down-field core and the continuum. Thus a remarkable enhancement of the ionization probability happens around the critical distance R_c. According to the intuitive physical picture, electron wave-packet direct ionization from the up-field site (DIU) is considered responsible for molecular EI.

Although such a DIU physical picture has been commonly used to analyze and explain the experiments of molecular ionization and related processes [21], the physical picture of molecular EI is still unclear and confusing. For instance, in [22], Betsch *et al.* measured the ejection direction of multiple charged ion fragments from a variety of molecules (N_2, O_2, CO, CO_2, and HBr) driven by a two-color laser field. The observed forward-backward dissociation asymmetries may imply that the electron is preferentially emitted from the down-field site, in contradiction with the DIU physical picture. Recently, a single-color elliptically polarized laser pulse was used to probe the tunneling site of electrons from the dimer ArXe [23] by the angular streaking technique [24]. Wu *et al.* [23] reported that the ionization more easily happens at the up-field site, supporting the DIU physical picture. Because the intuitive physical picture is based on the quasistatic theory, lacking a perspective on the dynamics of ionization processes, controversy still exists in these experiments.

To understand the long-standing issues about EI [22,23,25–27], in this work, we investigate the electron dynamics and the tunneling site by carefully examining the time evolution of the electron density and ionization rate by numerically solving the time-dependent Schrödinger equation (TDSE). A more comprehensive physical picture is established for EI dynamics of diatomic molecules. Besides the DIU ionization channel, we find another two ionization channels. The contributions from these channels depend on the asymmetry and internuclear distance of the molecules.

II. THEORETICAL MODEL

This work is intended to explore a general effect, rather than to model a special experiment and a special molecular target, so we consider a generic model diatomic molecule aligned along the electric-field vector of the linearly polarized light. We employ the two-dimensional TDSE model, which has been widely used for a reliable representation of molecular dynamics [28]. The TDSE of the diatomic molecule can be written as [atomic units (a.u.) are used throughout this paper

*Corresponding author: pengfeilan@hust.edu.cn
†Corresponding author: lupeixiang@mail.hust.edu.cn

unless stated otherwise]

$$i\frac{\partial\psi(x,y,t)}{\partial t}=\left[-\frac{1}{2}\nabla^2+V(x,y,t)\right]\psi(x,y,t), \quad (1)$$

where $\nabla^2=\frac{\partial^2}{\partial x^2}+\frac{\partial^2}{\partial y^2}$, and x and y denote the electron coordinates. $V(x,y,t)$ is the combined Coulomb and laser field potentials and reads

$$V(x,y,t)=-\frac{Z_1}{\sqrt{(x+R/2)^2+y^2+a}}-\frac{Z_2}{\sqrt{(x-R/2)^2+y^2+b}}+xE(t). \quad (2)$$

R is the internuclear distance. Z_1 and Z_2 are the electric charges of two nuclei, which are fixed at $(-R/2,0)$ and $(+R/2,0)$, respectively. a and b are the screening parameters of the left and right nuclei. $E(t)=E_0\sin^2(\pi t/\tau_p)\cos(\omega t)$ is the electric field of the laser pulse, with the angular frequency $\omega=0.057$ a.u. (corresponding to the wavelength 800 nm) and the full duration $\tau_p=10T$ (T is the laser cycle). In this work, we change the parameters Z_1, Z_2, a, and b to investigate the role of the molecular asymmetry on enhanced ionization. Here the molecular asymmetry is defined by the parameter $A=I_{pl}/I_{pr}$, where I_{pl} and I_{pr} denote the ionization energies of the left and the right cores, respectively, when the neighboring core is removed. We chose a set of parameters $Z_1=2$, $Z_2=1$, $a=0.5$, and $b=0.5$ to represent a model molecule with large asymmetry (e.g., HeH^{2+}). According to the definition above, the asymmetry parameter is $A=1.38/0.54=2.6$. The other set of parameters $Z_1=1$, $Z_2=1$, $a=0.39$, and $b=0.92$ is used to represent a model molecule with small asymmetry (e.g., $ArXe^{+}$). Its asymmetry parameter is $A=0.58/0.45=1.3$. In our work the laser intensity of 1×10^{15} W/cm^2 is used for the former molecule, and 9×10^{13} W/cm^2 is used for the latter molecule.

Initially, the system is in its ground state, which is calculated via imaginary-time propagation. Then the wave function of the system is propagated exactly in the presence of combined Coulomb and laser field potentials. We use the split-operator spectral method [29] to numerically solve the TDSE of the diatomic molecule. In this work the symmetrically second-order split operator algorithm is used. It can be expressed formally as

$$\psi(x,y,t+\Delta t)=\exp\left(\frac{i\Delta t\nabla^2}{4}\right)\exp\left[-i\Delta tV\left(x,y,t+\frac{\Delta t}{2}\right)\right]\times\exp\left(\frac{i\Delta t\nabla^2}{4}\right)\psi(x,y,t)+O[(\Delta t)^3]. \quad (3)$$

The commutation errors give rise to the third-order term in Δt. Equation (3) shows that the time propagation of the wave function from t to $t+\Delta t$ is achieved by three steps.

(i) First the operator $\exp(i\Delta t\nabla^2/4)$ applied to $\psi(x,y,t)$ is equivalent to a free particle propagation over a half-time increment $\Delta t/2$. This procedure is implemented with the help of the fast Fourier transform algorithm, which is very efficient and accurate.

(ii) Then the wave function gets a phase change from the action of the potential applied over the whole increment Δt.

(iii) Finally there is an additional free particle propagation over a half-time increment $\Delta t/2$. In this way the time propagation of the wave function is achieved from the beginning to the end of the laser field. In order to clarify the ultrafast electron dynamics in the enhanced ionization process we need to carefully examine the time evolution of the ionization rate and the electron density. We first calculated the probability flux at $x=-R/2-9$ and $R/2+9$. They represent the ionization rates from the left ($x<0$) and right ($x>0$) sides, respectively. Furthermore, by integrating the ionization rates from the beginning to the end of the laser pulse, the ionization probabilities from the left and right sides are obtained. Moreover, we record the wave function at each time and integrate over the y axis. In this way we obtain the dynamical evolution of the electron density of the molecular system in the laser polarization direction (x direction), which is very effective for the study of the detailed dynamics of the electron.

In our calculation the numerical grid is from -51.0 to 51.0 a.u. along each axis with a spacing of 0.2 a.u. In order to avoid the effect of rescattering on the flux calculations, we absorbed the ionizing wave packets soon after they left the parent ions by using a $\cos^{1/2}$-mask function set over $|x|>20.0$ a.u. To confirm the simulation and examine the influence of the rescattering wave packet, we also carried out test simulations by enlarging the grid region to $[-102,102]$ a.u. and setting the mask function over the region $|x|>85.0$ a.u., which is much larger than the quiver radius of the electron [30] in the laser field of 10^{15} W/cm^2. Therefore, the rescattering wave packet can be well included in the test simulations. The results show that the differences between the simulations with small and large grid regions are negligible.

III. RESULTS AND DISCUSSIONS

Figures 1(a) and 1(b) show the ionization probabilities as a function of internuclear distance R for the molecules with large and small asymmetries, respectively. The blue and red curves show the ionization probabilities from the left ($x<0$) and right ($x>0$) sides, which are obtained by integrating the probability flux at $x=-R/2-9$ and $R/2+9$ from the beginning to the end of the laser pulse. The green curve represents the total ionization probability. With the increase of R, the total ionization probabilities for both of these two molecules first increase and then gradually decrease.

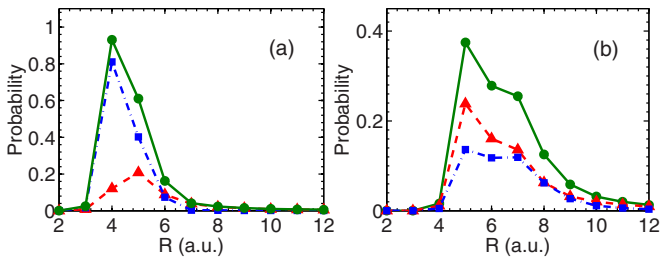

FIG. 1. (Color online) Total (green), left (blue), and right (red) ionization probabilities as a function of internuclear distance R. (a) The molecule with large asymmetry. (b) The molecule with small asymmetry.

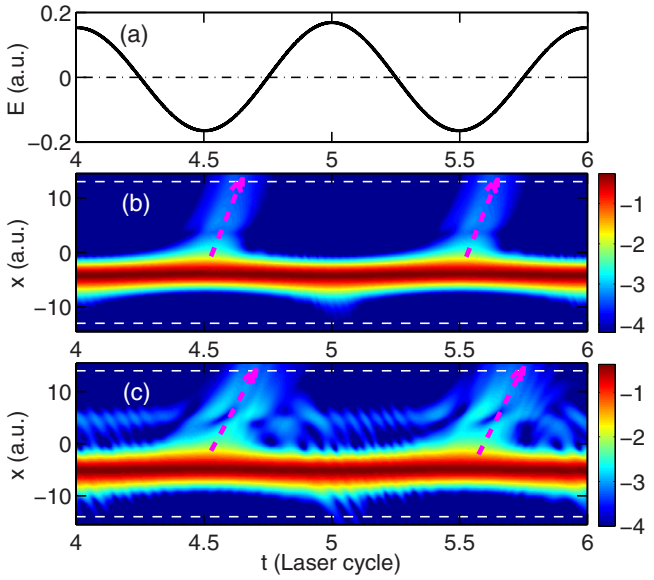

FIG. 2. (Color online) (a) The laser electric field. (b) and (c) Electron density as a function of time and the coordinate x for the molecule with large asymmetry at $R = 8$ a.u. and for the molecule with small asymmetry at $R = 10$ a.u.

A remarkable enhancement happens around $R = 4$ and 6 a.u. for the molecule with large asymmetry [see Fig. 1(a)] and small asymmetry [see Fig. 1(b)], respectively. However, one can see a distinct difference between these two molecules. For the molecule with large asymmetry, the probability of electrons escaping from the left side is much larger than that from the right side around the critical distance, whereas for the molecule with small asymmetry the ionization probability from the left side is slightly smaller than that from the right side around the critical distance. At large internuclear distance ($R > 8$), both molecules show slightly more electrons emitted from the right side.

In order to explore if the electron is emitted from the up-field site or down-field site, we carefully examine the time evolution of the electron density along the polarization direction. We first discuss the EI at large internuclear distance. Figures 2(b) and 2(c) show the electron density as a function of time for the molecule with large asymmetry at $R = 8$ a.u. and for the molecule with small asymmetry at $R = 10$ a.u., respectively. Recall that the electron is preferentially emitted from the right side at these internuclear distances as shown in Fig. 1. From Figs. 2(b) and 2(c) one can see that the ionization mainly occurs at the two instants around $t = 4.5T$ and $5.5T$. At those times, the electric field is negative and thus the left core is up field. The result indicates that the electron wave packet located at the left (i.e., up-field) core directly tunnels through the inner potential barrier to the continuum. This ionization channel, the so-called direct ionization from the up-field site (DIU), is consistent with the intuitive physical picture of molecular EI. Therefore, for asymmetric diatomic molecules DIU is the dominant ionization channel at large internuclear distance.

Next, we discuss the ionization dynamics at relatively small internuclear distance. Figure 3(b) shows the ionization rate from the left (blue curve) and right (red curve) sides as a function of time for the molecule with large asymmetry at

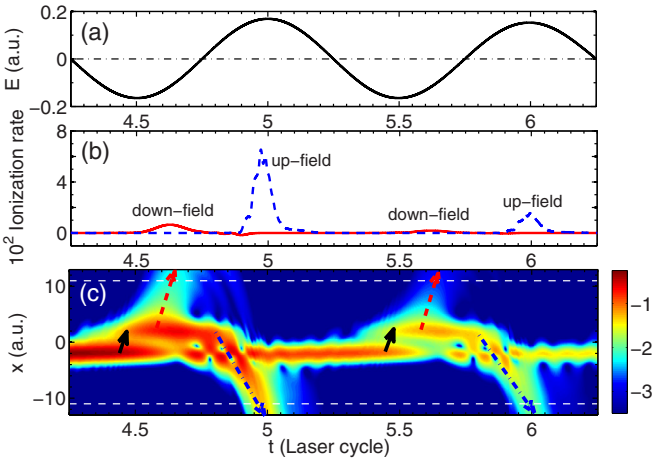

FIG. 3. (Color online) (a) The laser electric field. (b) Ionization rate from the left (blue) and right (red) sides as a function of time. (c) Electron density as a function of time and the coordinate x and the molecule with large asymmetry at $R = 4$ a.u.

$R = 4$ a.u. One can see that the dominant ionization burst is from the left side around $t = 5.0T$, when the electric field is positive. There are also some electron wave packets escaping away from the right side with low probabilities around $t = 4.65T$ and $5.65T$ and from the left side around $t = 6.0T$. In order to more clearly reveal the dynamics of electron emissions, the time evolution of the electron density is examined. As shown in Fig. 3(c), the molecule is initially at the ground state and the electron wave packet is dominantly localized at the left core. At the instant of $t = 4.45T$, some electron population is first excited to the right core [15], as indicated by the black arrow. A short time later, at the instant of $t = 4.6T$ a small part of the excited population leaves from the right core (see the red arrow). When this electron wave packet arrives at $x = 11$ a.u. (the white dashed curve), it is considered that ionization occurs. At this time the electric field is still negative and thus the right core is down field. That is to say, the electron escapes away from the down-field site by this process. Furthermore, the more excited population remains localized at the right core. When the electric field becomes positive and the right core is promoted to the up-field site, the excited population quickly tunnels through the inner potential barrier to the continuum around $t = 5.0T$ (see the blue arrow), which corresponds to the highest ionization peak in Fig. 3(b). In this channel the electron is emitted from the up-field site. Different from the DIU channel at large R, the ionization channel at small R mentioned above is a two-step process. The first step is that the electron population located at the left core is excited to the right core when the electric field is negative. Then the excited electron wave packet can be ionized by two paths. One path is that the excited electron wave packet tunnels through the right outer potential barrier to ionize from the down-field site when the electric field is negative. The other path is that the excited electron wave packet stays until the electric field reverses and then goes through the inner potential barrier to directly ionize from the up-field site. Moreover, for large asymmetric molecules, there is a more excited electron population ionized from the up-field site.

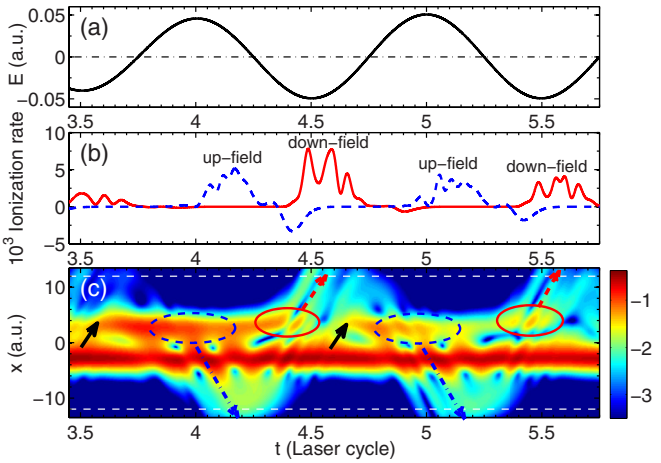

FIG. 4. (Color online) (a) The laser electric field. (b) Ionization rate from the left (blue) and right (red) sides as a function of time. (c) Electron density as a function of time and the coordinate x and the molecule with small asymmetry at $R = 6$ a.u.

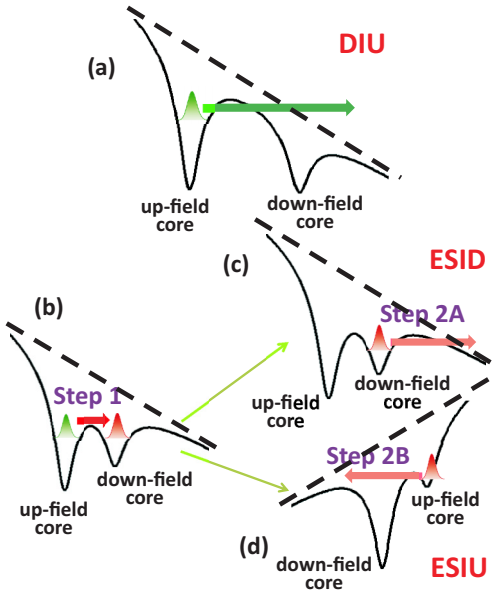

FIG. 5. (Color online) Sketches of the three different ionization channels.

Further, we analyze the ionization dynamics for small asymmetric molecules. Figure 4 shows the ionization rate from the left (blue curve) and right (red curve) sides and the electron density along the polarization direction as a function of the time for the molecule with small asymmetry at $R = 6$ a.u. Due to the periodicity of the ionization signal, we only need to analyze the region from $4.6T$ to $5.7T$. One can see that a part of the electron population is excited to the right core at $t = 4.6T$ (see the black arrow). Then the electric field turns positive at $t = 4.75T$ and within the subsequent positive half cycle $[4.75T, 5.25T]$ a part of the excited electron population tunnels through the inner barrier to ionize from the left side (see the blue arrow). After the electric field reverses again at $t = 5.25T$, the right core is lowered to the down-field site. The residual excited population localized at the right core tunnels through the right outer barrier to the continuum around $t = 5.5T$ (see the red arrow). Similar to the molecule with large asymmetry, these two ionization channels are also a two-step process. The only difference is that the excited electron population emitted from the down-field site stays at the right core for a longer time. The emitted electrons from the left and right sides correspond to the ionization of the up-field and down-field sites, respectively. Furthermore, we integrate the ionization rate from the left and the right sides shown in Fig. 4(b) over time. The result reveals that the ionization probability from the right side is slightly larger than that from the left side. That is to say, the excited electron population is more likely ionized from the down-field site, which is opposite to the case of the molecule with large asymmetry and also in contradiction with the DIU physical picture. This result indicates that the tunneling site in EI depends on the molecular asymmetry.

In addition, as compared with the molecule with large asymmetry, the ionization rate curves for the molecule with small asymmetry are wider, as shown in Figs. 2(c) and 4(b). Moreover, one can see multiple peaks in the ionization rate curves. A similar multiple-peak structure within a half cycle of the laser field has also been found for H_2^+ in [31] and attributed to the transient localization of the electron at one of the nuclei [32]. In Fig. 4(c) a similar transient localization of the electron is also visible and results in a wider time distribution of the ionization signal.

Our results suggest that the following scenario takes place for EI of diatomic molecules. There are three main ionization channels, as shown in Fig. 5. At large internuclear distance, the electron located at the left core directly tunnels through the inner potential barrier between the two cores to the continuum, as shown in Fig. 5(a). This ionization channel, electron wave-packet direct ionization from the up-field site (DIU), is consistent with the intuitive physical picture for the molecular EI. As the internuclear distance decreases, the contribution from the DIU channel quickly decreases. At small internuclear distance, the other two ionization channels dominate. Both of the two channels are two-step processes, and their first step is the same. The first step is that the electron population located at the left core is excited to the right core when the electric field is negative [see Fig. 5(b)]. Then the excited electron wave packet can be emitted by two paths. One path is that the excited electron wave packet around the right core tunnels through the right outer barrier to the continuum when the electric field is negative. In this case the right core is down field [see Fig. 5(c)]. Thus this ionization channel can be called field-induced excitation with subsequent ionization from the down-field site (ESID). The other path is that the excited electron wave packet stays until the electric field turns positive. Then the excited electron wave packet tunnels through the inner potential barrier directly to the continuum. This ionization channel is referred to as field-induced excitation with subsequent ionization from the up-field site (ESIU), as shown in Figs. 5(b) and 5(d). Furthermore, for the molecule with large asymmetry (e.g., $A = 2.6$ in Fig. 3), ESIU is the dominant ionization channel. The relative contribution from the ESID channel gradually increases with decreasing molecular asymmetry and becomes comparable to ESIU when A is around 1.5–1.7. For the molecule with small asymmetry ($A < 1.5$), ESID will

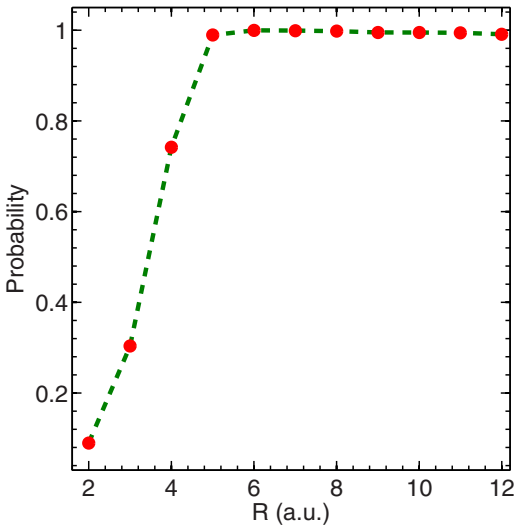

FIG. 6. (Color online) Ionization probability as a function of the internuclear distance R. The initial state is π orbital.

become the dominant ionization channel (e.g., $A = 1.3$ in Fig. 4).

As shown in Figs. 2–4, there exists an apparent time difference between the electron emissions by the three ionization channels. Due to the existence of the ionization time difference, an elliptically (or circularly) polarized laser pulse can drag those electrons from different channels to different directions. Therefore the angular resolved photoelectron spectra with an elliptically (or circularly) polarized pulse can be regarded as experimental observables to identify different ionization channels.

In the above discussion, the initial states of the systems are σ orbitals. We further consider adopting the π orbital as the initial state. Here we take the highest occupied molecular orbital (HOMO) of HBr, for example. Its orbital is simulated by solving the TDSE as in [33]. In order to well reproduce the ionization energy (0.43 a.u.) of the HOMO of HBr at equilibrium distance ($R = 2.67$ a.u.), the corresponding parameters are set as $Z_1 = 1.2$, $Z_2 = 0.6$, $a = 0.7$, and $b = 0.7$. The result is shown in Fig. 6. One can see that the ionization probability increases with increasing R from 2 to 5 a.u. and the ionization saturates when $R > 5$ a.u. Thus one cannot find the critical distance R_c at which the ionization yield is maximum. In other wards, EI is not observed for the initial state of the π orbital, which is similar to the case of the $2p\pi$ state of H_2^+ [33]. This is possibly because there is no electron distribution along the molecular axis for the π-type orbital.

IV. CONCLUSIONS

In conclusion, we have investigated the dynamics of electron emissions in strong-field EI of diatomic molecules by numerically solving the TDSE. It is found that there are three ionization channels leading to ionization enhancement. Their relative contributions are related to the molecular asymmetry and internuclear distance. At large internuclear distance the dominant contribution is from the DIU ionization channel regardless of molecular asymmetry, which is consistent with the intuitive physical picture of EI. However, at small internuclear distance the other two ionization channels dominate and their relative contributions depend on the molecular asymmetry. For the molecule with large asymmetry the electron is preferentially ionized from the up-field site by the ESIU channel, whereas for the molecule with small asymmetry the electron is more likely ionized from the down-field site by the ESID channel. Our work provides a more comprehensive physical picture for EI of diatomic molecules. It can promote the understanding of the dissociation dynamics of molecules.

ACKNOWLEDGMENTS

This work was supported by the National Natural Science Foundation of China under Grants No. 61275126 and No. 11234004 and the 973 Program of China under Grant No. 2011CB808103. Numerical simulations presented in this paper were partially carried out using the High Performance Computing Center experimental testbed in SCTS/CGCL (see http://grid.hust.edu.cn/hpcc).

[1] M. Hentschel, R. Kienberger, Ch. Spielmann, G. A. Reider, N. Milosevic, T. Brabec, P. Corkum, U. Heinzmann, M. Drescher, and F. Krausz, Nature (London) **414**, 509 (2001).

[2] F. Krausz and M. Ivanov, Rev. Mod. Phys. **81**, 163 (2009).

[3] D. N. Fittinghoff, P. R. Bolton, B. Chang, and K. C. Kulander, Phys. Rev. Lett. **69**, 2642 (1992).

[4] W. Becker, X. Liu, P. J. Ho, and J. H. Eberly, Rev. Mod. Phys. **84**, 1011 (2012).

[5] G. G. Paulus, W. Nicklich, H. Xu, P. Lambropoulos, and H. Walther, Phys. Rev. Lett. **72**, 2851 (1994); Y. Zhou, C. Huang, Q. Liao, and P. Lu, *ibid.* **109**, 053004 (2012).

[6] W. Becker, F. Grasbon, R. Kopold, D. B. Milošević, G. G. Paulus, and H. Walther, Adv. At. Mol. Opt. Phys. **48**, 35 (2002).

[7] D. Pavičić, K. F. Lee, D. M. Rayner, P. B. Corkum, and D. M. Villeneuve, Phys. Rev. Lett. **98**, 243001 (2007); A. S. Alnaser, S. Voss, X. M. Tong, C. M. Maharjan, P. Ranitovic, B. Ulrich, T. Osipov, B. Shan, Z. Chang, and C. L. Cocke, *ibid.* **93**, 113003 (2004); R. Murray, M. Spanner, S. Patchkovskii, and M. Y. Ivanov, *ibid.* **106**, 173001 (2011); Y. Li, X. Zhu, P. Lan, Q. Zhang, M. Qin, and P. Lu, Phys. Rev. A **89**, 045401 (2014).

[8] G. L. Kamta and A. D. Bandrauk, Phys. Rev. A **74**, 033415 (2006); M. Meckel *et al.*, Science **320**, 1478 (2008).

[9] A. M. Perelomov, V. S. Popov, and M. V. Terent'ev, Sov. Phys. JETP **23**, 924 (1966).

[10] M. V. Ammosov, N. B. Delone, and V. P. Kralnov, Sov. Phys. JETP **64**, 1191 (1986).

[11] X. M. Tong and C. D. Lin, J. Phys. B **38**, 2593 (2005).

[12] K. Codling, L. J. Frasinski, and P. A. Hatherly, J. Phys. B **22**, L321 (1989); K. Codling and L. J. Frasinski, *ibid.* **26**, 783 (1993).
[13] T. Seideman, M. Y. Ivanov, and P. B. Corkum, Phys. Rev. Lett. **75**, 2819 (1995).
[14] T. Zuo and A. D. Bandrauk, Phys. Rev. A **52**, R2511 (1995); S. Chelkowski and A. D. Bandrauk, J. Phys. B **28**, L723 (1995).
[15] G. L. Kamta and A. D. Bandrauk, Phys. Rev. Lett. **94**, 203003 (2005).
[16] M. Schmidt, D. Normand, and C. Cornaggia, Phys. Rev. A **50**, 5037 (1994).
[17] D. Normand and M. Schmidt, Phys. Rev. A **53**, R1958 (1996).
[18] E. Constant, H. Stapelfeldt, and P. B. Corkum, Phys. Rev. Lett. **76**, 4140 (1996).
[19] G. N. Gibson, M. Li, C. Guo, and J. Neira, Phys. Rev. Lett. **79**, 2022 (1997).
[20] N. B. Delone and V. P. Krainov, J. Opt. Soc. Am. B **8**, 1207 (1991).
[21] D. Pavičić, A. Kiess, T. W. Hänsch, and H. Figger, Phys. Rev. Lett. **94**, 163002 (2005).
[22] K. J. Betsch, D. W. Pinkham, and R. R. Jones, Phys. Rev. Lett. **105**, 223002 (2010).
[23] J. Wu, M. Meckel, L. Ph. H. Schmidt, M. Kunitski, S. Voss, H. Sann, H. Kim, T. Jahnke, A. Czasch, and R. Dörner, Nat. Commun. **3**, 1113 (2012).
[24] P. Eckle, M. Smolarski, P. Schlup, J. Biegert, A. Staudte, M. Schöffler, H. G. Muller, R. Dörner, and U. Keller, Nat. Phys. **4**, 565 (2008).
[25] B. Sheehy, B. Walker, and L. F. DiMauro, Phys. Rev. Lett. **74**, 4799 (1995).
[26] M. R. Thompson, M. K. Thomas, P. F. Taday, J. H. Posthumus, A. J. Langley, L. J. Frasinski, and K. Codling, J. Phys. B **30**, 5755 (1997).
[27] D. Ray, F. He, S. De, W. Cao, H. Mashiko, P. Ranitovic, K. P. Singh, I. Znakovskaya, U. Thumm, G. G. Paulus, M. F. Kling, I. V. Litvinyuk, and C. L. Cocke, Phys. Rev. Lett. **103**, 223201 (2009).
[28] A. Picón, A. Jaroń-Becker, and A. Becker, Phys. Rev. Lett. **109**, 163002 (2012).
[29] M. Feit, J. Fleck, Jr., and A. Steiger, J. Comput. Phys. **47**, 412 (1982); P. Lan *et al.*, New J. Phys. **13**, 063023 (2013); P. Lan, P. Lu, W. Cao, X. Wang, and G. Yang, Phys. Rev. A **74**, 063411 (2006); C. Huang *et al.*, J. Opt. Soc. Am. B **29**, 734 (2012).
[30] P. B. Corkum, Phys. Rev. Lett. **71**, 1994 (1993).
[31] N. Takemoto and A. Becker, Phys. Rev. Lett. **105**, 203004 (2010).
[32] I. Kawata, H. Kono, and Y. Fujimura, J. Chem. Phys. **110**, 11152 (1999).
[33] G. L. Kamta and A. D. Bandrauk, Phys. Rev. A **75**, 041401(R) (2007).